ACCSCIENCE PUBLISHING

Eurasian Journal of Medicine and Oncology

ORIGINAL RESEARCH ARTICLE

Evaluation of the efficiency of double recombinant vaccinia virus VV-GMCSF-Lact against glioblastoma using 3D spheroid and cerebral organoid models

Maya Dymova[1†*], Gleb Petrov[1†], Danil Drokov[1], Tatiana Shnaider[2], Sophia Yakovleva[2], Elena Kuligina[1], and Vladimir Richter[1]

[1]Laboratory of Biotechnology, Institute of Chemical Biology and Fundamental Medicine, Siberian Branch of the Russian Academy of Sciences, Novosibirsk, Novosibirsk Region, Russia

[2]Department of Molecular Mechanisms of Ontogenesis, Institute of Cytology and Genetics, Siberian Branch of the Russian Academy of Sciences, Novosibirsk, Novosibirsk Region, Russia

[†]*These authors contributed equally to this work.*

***Corresponding author:**
Maya Dymova
(dymova@1bio.ru)

Citation: Dymova M, Petrov G, Drokov D, *et al*. Evaluation of the efficiency of double recombinant vaccinia virus VV-GMCSF-Lact against glioblastoma using 3D spheroid and cerebral organoid models. *Eurasian J Med Oncol*. 2026;10(2):025440462. doi: 10.36922/EJMO025440462

Received: November 1, 2025

Revised: December 11, 2025

Accepted: January 14, 2026

Published online: February 20, 2026

Abstract

Introduction: Human cerebral organoids (COs) are sophisticated three-dimensional (3D) models that successfully replicate the 3D cytoarchitecture of human brain development in its early stages. Co-cultivation of COs obtained from human-induced pluripotent stem cells with 3D U-87 MG glioblastoma cell spheroids (glioblastoma–CO assembloid [GCOA]) represents a robust strategy for modeling brain cancer behavior.

Objectives: This study aims to evaluate the feasibility of using GCOAs and 3D U-87 MG glioblastoma cell spheroids as *in vitro* cell models to evaluate the cytotoxic effect of the oncolytic recombinant vaccinia virus-granulocyte–macrophage colony-stimulating factor (VV-GM-CSF)-Lact compared to the VV-GMCSF-del virus.

Methods: To assess the cytotoxicity of two virus strains, we used fluorescent and confocal microscopy, spectrophotometry, the MTT assay, and real-time polymerase chain reaction

Results: Glioblastoma cells died faster in the presence of VV-GMCSF-Lact virus, and 3D spheroids infected with this virus contained more caspase-3-positive cells. On the 10th day in GCOA, glioblastoma cells began to invade the interior of the CO. Under conditions of 3D spheroid and GCOA infection with recombinant viruses, three differentially expressed genes – *FSCN1, SCUBE2,* and *TNFRSF9* – associated with invasion were analyzed.

Conclusion: These 3D models of glioblastoma can be used in the development of antitumor drugs to study their cytotoxic effects.

Keywords: Glioblastoma; Cerebral organoids; Three-dimensional spheroids; Glioblastoma–cerebral organoid assembloid; VV-GMCSF-Lact; Oncolytic virus

1. Introduction

Although malignant brain and other central nervous system (CNS) tumors make a relatively small contribution to the structure of tumor diseases, they are among the most devastating and deadly neoplasms. According to the latest data, there were 321,476 new cases of brain and other CNS cancers and 248,305 deaths from these malignancies worldwide in 2022.[1] Glioblastoma, a highly aggressive Grade IV glioma, accounts for approximately 49% of all primary brain tumors and has an extremely poor prognosis for patients, with median overall survival ranging from 14 to 20.9 months from initial diagnosis.[2] Despite recent advances in the standard treatment of glioblastoma, which includes maximal surgical resection and adjuvant chemoradiotherapy, the 5-year relative survival rate for patients remains below 10%.[3]

Along with intrinsic tumor heterogeneity, cancer stem cells, and immune evasion, the highly infiltrative nature of glioblastoma is considered a major factor contributing to this devastating patient prognosis.[4-6] The invasion of glioblastoma cells to distant healthy tissues has been shown to result in insufficient tumor resection, almost inevitably causing tumor recurrence from remaining cancer cells after primary treatment.[7] Previous studies assessing the expression of genes associated with tumor proliferation and invasion have demonstrated their association with patient prognosis; therefore, defining the repertoire of differentially expressed genes and identifying potential target genes among them may be promising for the development of antitumor drugs.[8,9]

Three-dimensional (3D) *in vitro* cell systems have emerged as a promising means of cancer modeling, overcoming the inability of two-dimensional (2D) cell cultures to recapitulate morphological, genetic, and proteomic characteristics of *in vivo* tumors and their stroma, as well as providing greater experimental access and throughput compared with animal models.[10] These models range widely from co-cultures of different cell types sustained in an extracellular matrix-mimicking scaffold to complex organotypic cultures obtained by seeding cancer cells into human brain slices.[11] Among these, 3D spheroids have been the predominant platform in the development of experimental therapeutic approaches to human glioblastoma. Obtained by aggregating cancer cells in a scaffold-free manner, spheroids are capable of reproducing the intricate architecture of solid tumors while successfully mimicking the patterns of oxygen, nutrients, and therapeutic agent penetration and distribution observed in tumors *in situ*. At the same time, despite the possibility of co-culturing cancer cells and nonmalignant stromal and immune cells in the process of spheroid formation, this technology is far from being physiologically relevant and cannot be considered self-sufficient in studying the invasive characteristics of glioblastoma, requiring a hydrogel or Matrigel scaffold to simulate distant parts of the brain parenchyma.[12]

More sophisticated and advanced glioblastoma modeling strategies use human cerebral organoids (COs), which successfully replicate the 3D cytoarchitecture of the early stages of human brain development.[13] Derived from stem cells, COs represent a complex, self-assembly of neurons and neural cells, including radial and basal radial glia, and may serve as a unique platform for studying multiple characteristics of brain cancer.[14,15] One promising existing model based on this technology uses targeted activation of oncogenic mutations in CO cells to recapitulate the earliest stages of glioblastoma development.[16,17] Co-cultivation of COs with cancer cell spheroids represents another reliable strategy for modeling brain cancer behavior.[18] The neuroanatomically realistic structure of COs has been shown to promote the formation of a realistic tumor microenvironment when co-cultured with patient-derived glioblastoma cells, which in turn facilitates the reproduction of patient-specific tumor phenotypic and transcriptomic characteristics.[15,19] Moreover, it has been demonstrated that COs have the potential to even alter the gene expression profile of an immortalized glioblastoma cell line, inducing its transition towards an *in vivo* phenotype.[20]

In this work, we used co-cultivation of COs derived from human-induced pluripotent stem cells (hiPSCs) with glioblastoma spheroids (glioblastoma–CO assembloid [GCOA]) and 3D U-87 MG glioblastoma cell spheroids as *in vitro* cell models to study the cytotoxic effects of the oncolytic virus VV-GMCSF-Lact. This double recombinant vaccinia virus granulocyte–macrophage colony-stimulating factor (VV-GMCSF)-Lact, developed jointly by the Institute of Chemical Biology and Fundamental Medicine, Siberian Branch of the Russian Academy of Sciences and the State Research Center of Virology and Biotechnology Vector, has completed the first phase of clinical trials for the treatment of breast cancer (ClinicalTrials.gov identifier: NCT05376527) and is a promising, highly effective treatment for glioblastoma.[21] VV-GMCSF-Lact features deletions in viral thymidine kinase and growth factor genes, which are replaced with human genes encoding GM-CSF and the oncotoxic protein lactaptin, whose expression has been shown to reinforce the antitumor efficiency of the virus.[22] As a control, we used the virus VV-GMCSF-del, in which the lactapin gene is deleted. Although previous studies using traditional 2D cell cultures and orthotopic mouse models succeeded

in demonstrating the high cytotoxicity and selectivity of VV-GMCSF-Lact against human glioblastoma,[23] data on the effects of infection with these oncolytic viruses on 3D models of glioblastoma and tumor cell invasion processes are still limited.

Therefore, the present study aims to:

(i) Establish a 3D glioblastoma cellular model based on GCOA that would mimic the cytoarchitecture of the brain, including a bulk tumor and the invasion of tumor cells into the depth of the cerebral spheroid.
(ii) Evaluate the expression of genes associated with tumor cell proliferation and invasion.
(iii) Compare the oncolytic efficacy and the effect on invasion of VV-GMCSF-Lact and VV-GMCSF-del in the developed 3D models.

2. Materials and methods

2.1. Cell culture

The glioblastoma U-87 MG cell line transduced with a lentivirus carrying the *GFP* gene was obtained from the Cell Culture Collection of Institute of Chemical Biology and Fundamental Medicine, Siberian Branch of the Russian Academy of Sciences, Novosibirsk, Russia, and was maintained in a complete growth medium (Dulbecco's Modified Eagle Medium/Nutrient Mixture F-12 [DMEM/F12] supplemented with 10% fetal bovine serum [Gibco, USA], 2 mM L-glutamine [Gibco, USA], and 1% [v/v] antibiotic–antimycotic solution [Gibco, USA]) in a humidified atmosphere containing 5% CO_2 at 37°C.

The hiPSC line iTAF1-36, derived from a healthy donor, was previously established and characterized.[24] Cells were maintained under feeder-free conditions in complete mTeSR™1 medium (STEMCELL Technologies, Canada) on plates coated with Corning® Matrigel® hESC-Qualified Matrix (Corning Life Sciences, USA) at 37°C and 5% CO_2. hiPSCs were passaged every 4–5 days and detached using StemPro™ Accutase™ Cell Dissociation Reagent (Thermo Fisher Scientific, USA).

2.2. Three-dimensional U-87 MG glioblastoma spheroid, CO, and GCOA generation

Three-dimensional U-87 MG glioblastoma cell spheroids were created using commercially available AggreWell™800 culture plates (STEMCELL Technologies, Canada). Cells were detached using 0.25% trypsin–ethylenediaminetetraacetic acid (EDTA; Gibco, USA) and seeded at 3×10^6 cells/well on plates pre-treated with anti-adherence rinsing solution (STEMCELL Technologies, Canada). After seeding, cells were cultured for 2 days to form spheroids and then transferred to 100 mm cell culture dishes for 30 days. Spheroids were cultivated at 80 rpm in the CO_2 incubator shaker (Radobio Scientific Co., Ltd., China) for continuous agitation. The growth medium was changed every 4 days.

COs were generated from hiPSCs according to the previously described protocol with minor modifications.[25] Briefly, 3×10^6 cells were seeded into AggreWell™800 plates coated with anti-adherence rinsing solution, and 20 μM Y-27632 (STEMCELL Technologies, Canada) was added to the embryoid body medium containing 80% DMEM/F12, 20% KnockOut™ Serum Replacement (Thermo Fisher Scientific, USA), 1 mM L-glutamine, 1% Minimum Essential Medium Non-Essential Amino Acids (MEM NEAA; Gibco, USA), 0.1 mM 2-mercaptoethanol (Thermo Fisher Scientific, USA), 4 ng/mL basic fibroblast growth factor (Thermo Fisher Scientific, USA), and 1% penicillin–streptomycin (Thermo Fisher Scientific, USA) to enhance cell survival.

On day 2, embryoid bodies were transferred to 6-well plates. On day 5, basic fibroblast growth factor was removed from the medium. On day 7, the medium was switched to neural induction medium consisting of DMEM/F12 with N-2 Supplement (Thermo Fisher Scientific, USA), 1 mM L-glutamine, 1% MEM NEAA, 0.1 mM 2-mercaptoethanol, 1% penicillin–streptomycin, and 1 μg/mL heparin (Sigma-Aldrich, USA). On day 11, COs were embedded in 10 μL Cultrex Reduced Growth Factor Basement Membrane Extract (R&D System, USA) and cultured in CO differentiation medium without Vitamin A (DMEM/F12–neurobasal medium 1:1, 0.5× N-2 supplement, 1× B-27 supplement minus Vitamin A [Thermo Fisher Scientific, USA], 1 mM L-glutamine, 1% MEM NEAA, 0.1 mM 2-mercaptoethanol, 1% penicillin–streptomycin, and 2.5 μg/mL insulin (Sigma-Aldrich, USA]) in anti-adherence-treated dishes. On day 15, COs were removed from the Cultrex extract and transferred to differentiation medium with Vitamin A (DMEM/F12–neurobasal medium 1:1, 0.5× N-2 supplement, 1× B-27 supplement [Thermo Fisher Scientific, USA], 1 mM L-glutamine, 1% MEM NEAA, 0.1 mM 2-mercaptoethanol, 1% penicillin–streptomycin, 2.5 μg/mL insulin, 0.8 mM ascorbic acid (FUJIFILM Wako Pure Chemical Corporation, JAPAN], and 20 mM N-2-hydroxyethylpiperazine-N-2-ethanesulfonic acid [HEPES; Capricorn Scientific, Germany]), and cultured on a CO_2 incubator shaker at 80 rpm with medium changes every 4 days.

For GCOA generation, U-87 MG 3D spheroids were washed with phosphate-buffered saline (PBS) and incubated with EDTA for 20 min. Individual spheroids and COs were embedded together in a drop of Cultrex to form assembloids. After 30 min, chimeric organoids were transferred to a CO_2 incubator at 37°C for 3 days without

agitation. Following this initial period, GCOAs were maintained on a shaker for up to 30 days.

2.3. Viral infection

To study the cytotoxic activity of VV-GMCSF-Lact 3D spheroids, glioblastoma spheroids were plated in 12-well Nunclon Sphera plates and treated with a virus suspension with a virus titer of 2×10^7 plaque-forming units (PFU)/mL in complete DMEM/F12 culture medium. The cytotoxic effects of the virus were analyzed at 24 and 72 h and on day 7 after viral infection.

2.4. Cell viability assay

To determine the cytotoxicity of VV-GMCSF-Lact in relation to adherent U-87 MG glioblastoma cell cultures, the 3-(4,5-dimethylthiazol-2-yl)-2,5-diphenyltetrazolium bromide (MTT) assay was employed. Cells were seeded in 96-well plates at a density of 5×10^3 cells per well. Following 48 h of incubation, cells were infected with VV-GMCSF-Lact at a multiplicity of infection ranging from 10 PFU/cell to 0.0012 PFU/cell at 37°C for 72 h. The medium was then removed, and 200 µL of Iscove's Modified Dulbecco's medium containing 0.5 mg/mL MTT reagent was added to each well. After 4 h of incubation, the medium and MTT were removed and replaced with 100 µL of dimethyl sulfoxide. The optical density was measured on a microplate reader Apollo LB 912 (Berthold Technologies, Germany) at a wavelength of 570 nm (reference wavelength = 620 nm). The percentage of viable cells was determined as the ratio of the mean absorption values of the infected cells to the values obtained for untreated control cells. The IC_{50} value was defined as the half-maximal inhibitory concentration.

The alterations in the fluorescent signal intensity of U-87 MG glioblastoma cells in response to oncolytic virus treatment were quantified using a CLARIOstar Plus plate reader (BMG Labtech, Germany). Briefly, cells were seeded into 96-well plates at a density of 9×10^3 cells per well and incubated overnight. On the subsequent day, cells were treated with either VV-GMCSF-del or VV-GMCSF-Lact at a concentration of 2×10^7 PFU/well and incubated at 37°C. Fluorescence microscopy analysis using Nikon Eclipse Ti (Nikon, Japan) and subsequent fluorescence intensity measurements were performed at control time points of 24 h, 72 h, and 7 days.

2.5. Immunohistochemical staining of 3D spheroids and GCOAs sections

After incubation of 3D spheroids of glioblastoma and GCOAs with recombinant viruses for 24 h, 72 h, and 7 days, 3D spheroids were washed three times in PBS to remove the viral suspension and transferred to a 0.05% sodium azide solution (Thermo Fisher Scientific, USA) in PBS for preservation. Samples were fixed in 4% paraformaldehyde for 1 h at room temperature (RT) and then incubated in 15% sucrose at RT for 4 h, followed by incubation in 30% sucrose overnight with constant agitation. GCOAs and 3D spheroids were then embedded in a 7.5% gelatine/10% sucrose solution (Thermo Fisher Scientific, USA), frozen using liquid nitrogen, and subjected to cryosectioning. Subsequently, the neurospheres were cut using a Cryostat Microtome HM 550 (Thermo Scientific, USA), and the resulting sections were placed on glass slides.

The obtained sections were washed three times with 200 µL of cold PBS. Then, 100 µL of primary antibodies against GM-CSF (AF-215-NA, R&D Systems, USA), VV (1:300; ab35219, Abcam, United Kingdom), and caspase-3 (CASP3; sc-7272, Santa Cruz Biotechnology, USA) (Table 1) in blocking buffer (2% bovine serum albumin [Sigma-Aldrich, USA], 0.2% Triton X-100 [Sigma-Aldrich, USA], and 5% fetal bovine serum) were added per well and incubated overnight at RT on a shaker at 150 rpm. The next day, the buffer with primary antibodies was removed, and the wells were washed three times with 200 µL of cold PBS. Then, 100 µL of secondary antibodies, including Donkey Anti-Rabbit IgG H&L (ab150075, Abcam, United Kingdom), Goat anti-Mouse IgG (H+L) Highly Cross-Adsorbed Secondary Antibody (A32727, Thermo Fisher Scientific, USA), for 2 h at RT on a shaker at 150 rpm. Afterward, the buffer with secondary antibodies was removed, and the wells were washed three times with 200 µL of cold PBS, each wash lasting 20 min. Stained and air-dried sections were treated with antifade solution, covered with coverslips, and visualized using a confocal fluorescence microscope (Olympus Fluoview FV3000, Olympus Corporation, Japan). CASP3-positive cells were visualized using a 60× objective lens, while the whole spheroid or GCOA were visualized using a 20× objective lens.

To assess the number of CASP3-positive cells, image analysis was performed using ImageJ (ImageJ 1.54d, Wayne Rasband [NIH], USA). Each of the two groups had three time points, each with three 3D spheroids; each 3D spheroid was represented by three regions of interest (ROIs), resulting in $n = 9$ ROIs per group (3 spheroids × 3 ROIs). For each ROI, the ratio of CASP3-positive cells to total cells was determined, and graphs were constructed based on the obtained ratios.

2.6. Quantitative polymerase chain reaction (qPCR)

To determine the dynamics of viral load changes, qPCR was used. Genomic DNA was isolated from cell cultures treated with an oncolytic virus using a DU Cells, Tissues, and Blood DNA isolation kit (D-Blood-50, Biolabmix, Russia)

Table 1. Antibodies used for immunohistochemical staining

Antibody	Manufacturer	Product code	Dilution
Human GM-CSF	R&D systems, United States	AF-215-NA	1:100
Anti-Vaccinia Virus Antibody	Abcam, United Kingdom	ab35219	1:300
Caspase-3 Antibody (E-8)	Santa Cruz Biotechnology, United States	sc-7272	1:200
Donkey Anti-Rabbit IgG H&L (Alexa Fluor® 647)	Abcam, United Kingdom	ab150075	1:500
Goat Anti-Mouse IgG (H+L) Highly Cross-Adsorbed Secondary Antibody, Alexa Fluor™ Plus 555	Thermo Fisher Scientific, United States	A32727	1:500

Abbreviations: GM-CSF: Granulocyte–macrophage colony-stimulating factor, IgG: Immunoglobulin G

according to the manufacturer's protocol. PCR reactions were performed with 2× BioMaster RT-qPCR SYBR Blue mix (Biolabmix, Russia) using 2.5 ng of genomic DNA and 0.3 μM of primers (E3L-F and E3L-R) in a final volume of 20 μL. qPCR conditions included initial denaturation at 95°C for 5 min, followed by 35 cycles of denaturation for 10 s at 95°C, annealing for 20 s at 60°C, and elongation for 10 s at 72°C. For qPCR analysis, standard VV-GMCSF-Lact DNA serial dilutions were prepared.

For reverse-transcription qPCR with specific primers (Table 2), total RNA was extracted from cell cultures (virus-treated and untreated 3D cell models) using the LRU RNA isolation kit (LRU-100-50, Biolabmix, Russia) according to the manufacturer's protocol. Each PCR reaction was prepared with 2× BioMaster RT-qPCR SYBR Blue mix (Biolabmix, Russia) with 50 ng of total RNA and 0.3 μM of primers in a final volume of 20 μL. The following thermal cycling profile was used: 30 min cDNA synthesis at 45°C, initialization at 95°C for 5 min, followed by 35 cycles of denaturation for 10 s at 95°C, annealing for 20 s at 60°C, and elongation for 10 s at 72°C for primers *GAPDH*, *HPRT1*, *FSCN1*, and *SCUBE2*, or annealing for 20 s at 65°C and elongation for 10 s at 72°C for *GAPDH*, *HPRT1*, and TNFRSF9 primers.

Quantitative PCR was performed using a CFX96 Touch Real-Time PCR Detection System, and Bio-Rad CFX Manager Software (version 2.0, Bio-Rad, USA) was used for data analysis. Each PCR reaction was run in triplicate.

2.7. Statistical analysis

Data are presented as the mean ± standard deviation of at least three replicates. Statistical analysis was performed using GraphPad Prism version 6.01 (GraphPad Software, USA). A two-way analysis of variance with Fisher's least significant difference test (for the viral load analysis in 3D glioblastoma spheroids) or Tukey's multiple comparison test (for all other experiments) was applied for comparisons of more than two data sets. A $p<0.05$ was considered indicative of a statistically significant difference.

Table 2. Sequences of primers used for real-time real-time RT-PCR analysis of RNA expression

Primer	Sequence
E3L-F	5'-CTGACGCAGAGATTGTGTGTG-3'
E3L-R	5'-GGTGACAGGGTTAGCATCTTTC-3'
FSCN1-F	5'-CAACATCAAAGACTCCACAGG-3'
FSCN1-R	5'-CCATAGGGGCGACAGGTG-3'
SCUBE2-F	5'-TATGATGAGGACTACCAGGAAC-3'
SCUBE2-R	5'-CAATACCCGACTGTGCTGAC-3'
TNFRSF9-F	5'-CAGTCCCTGTCCTCCAAATAG-3'
TNFRSF9-R	5'-AGTGTCCTGGCTCTCTCGC-3'
GAPDH-F	5'-GAAGGTGAAGGTCGGAGT-3'
GAPDH-R	5'-GAAGATGGTGATGGGATTTC-3'
HPRT-F	5'-CATCAAAGCACTGAATAGAAAT-3'
HPRT-R	5'-TATCTTCCACAATCAAGACATT-3'

3. Results

3.1. Cytotoxicity of VV-GMCSF-Lact against adherent U-87 MG cultures

We first evaluated the cytotoxic effect of recombinant viruses against adherent cultures of U-87 MG cells, previously transduced with a lentiviral construct carrying the *GFP* gene. The IC_{50} for the VV-GMCSF-Lact was 0.62 PFU/cell, with a correlation coefficient of $R = 0.91$, whereas the cytotoxic dose of VV-GMCSF-del was estimated as $IC_{50} = 50.1$ PFU/cell ($R = 0.62$).

For further experiments, the working titer of the oncolytic viruses was determined to be 2×10^7 PFU/mL, which is close to the concentration used previously for intratumoral injection in mouse models.[23] We observed a significant decline in the fluorescence intensity of cells grown in adherent conditions when exposed to that amount of virus (Figure 1).

The fluorescent signal intensity in VV-GMCSF-Lact-treated cells decreased to approximately 35% compared with control cells within the first 24 h of incubation. By

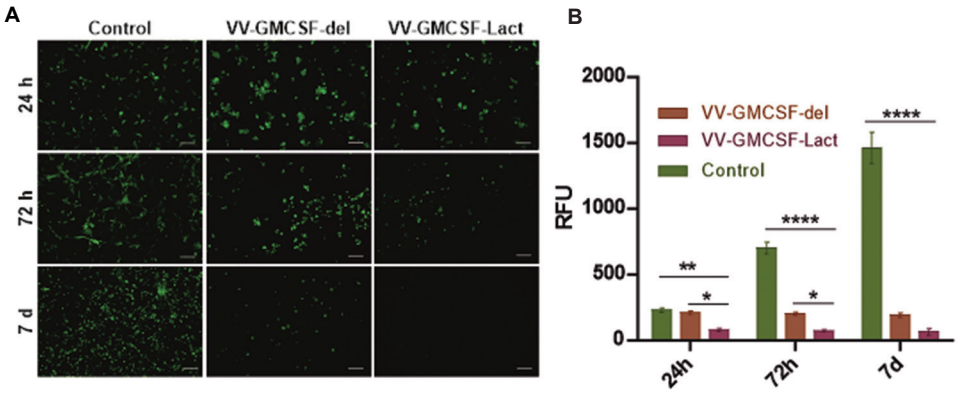

Figure 1. (A) Fluorescence microscopy image of adherent U-87 MG cells (scale bar: 100 μm; magnification: 20×) and (B) corresponding fluorescence intensity of cells infected with VV-GMCSF-Lact and VV-GMCSF-del viruses. *p<0.05, *p<0.01, ***p<0.001, and ****p<0.0001 indicate statistically significant different.
Abbreviations: RFU: Relative fluorescence unit; VV-GMCSF: Vaccinia virus-granulocyte–macrophage colony-stimulating factor.

day 7 of the experiment, the fluorescence signal intensity of cells infected with VV-GMCSF-del and VV-GMCSF-Lact was 14% and 7%, respectively, of the fluorescence level observed in control wells.

3.2. Viral load in three-dimensional glioblastoma spheroids

To evaluate the replication efficiency of recombinant viruses in 3D spheroids of glioblastoma, a set of primers targeting the interferon-resistance viral *E3L* gene was used. Using DNA samples extracted from serial dilutions of VV-GMCSF-Lact with concentrations ranging from 6.6×10^4 to 6.6×10^8 PFU/mL, we initially generated a qPCR standard curve. The quantification cycle values of the analyzed samples were then plotted onto the standard curve, and the number of VV-GMCSF-Lact and VV-GMCSF-del genomes was expressed as a PFU/mL (Figure 2). A decrease in viral titer was observed at day 7 for both viruses, but this was only a trend, and PFU/mL values adjusted for multiple comparisons were not significantly different.

As shown in Figure 2, the highest number of viral particles in spheroid cells was detected in the first 24 h of incubation and was 1.15×10^8 and 1.16×10^8 PFU/mL for VV-GMCSF-del and VV-GMCSF-Lact, respectively. On days 3 and 7, the concentration of VV-GMCSF-Lact in the analyzed samples was 1.15×10^8 and 3.68×10^7 PFU/mL, respectively. The decrease in the number of viral particles in glioblastoma spheroids by day 7, which was also observed for the single recombinant VV-GMCSF-del, is likely due to the progressive destruction of 3D cultures by the oncolytic virus.

3.3. Evaluation of the efficacy of recombinant viruses using immunohistochemical analysis

3.3.1. Immunohistochemical analysis of 3D spheroids incubated with VV-GMCSF-del and VV-GMCSF-Lact viruses

Three-dimensional spheroids incubated with VV-GMCSF-del and VV-GMCSF-Lact viruses were analyzed at 24 h, 72 h, and 7 days after cell infection. The following molecular markers were used for immunohistochemical analysis: B5R, GMCSF, and CASP3. B5R and GM-CSF were used to assess viral infection and GM-CSF transgene expression, respectively, and CASP3 was used to evaluate the level of apoptosis. After immunohistochemical staining, the obtained preparations were analyzed using a laser scanning confocal microscope using fluorescence isothiocyanate, 4',6-diamidino-2-phenylindole, Cyanine 5, and Alexa 546 filters (Figures 3 and 4).

The number of CASP3-positive cells in 3D spheroids was assessed after incubation with viruses for 24 h, 72 h, and 7 days (Figure 4B). The graph shows that the proportion of CASP3-positive cells remained at an approximately constant elevated level at all three time points in the VV-GMCSF-Lact group, whereas in the VV-GMCSF-del group, the proportion of CASP3-positive cells increased only at day 7 post-infection. The differences between the 24- and 72-h time points were statistically significant (p <0.0001).

3.3.2. Evaluation of 3D glioblastoma spheroid invasion into COs and the impact of infection on GCOAs

The expression profiles of several genes (*FSCN1, SCUBE2, TNFRSF9*) were examined to determine how they were

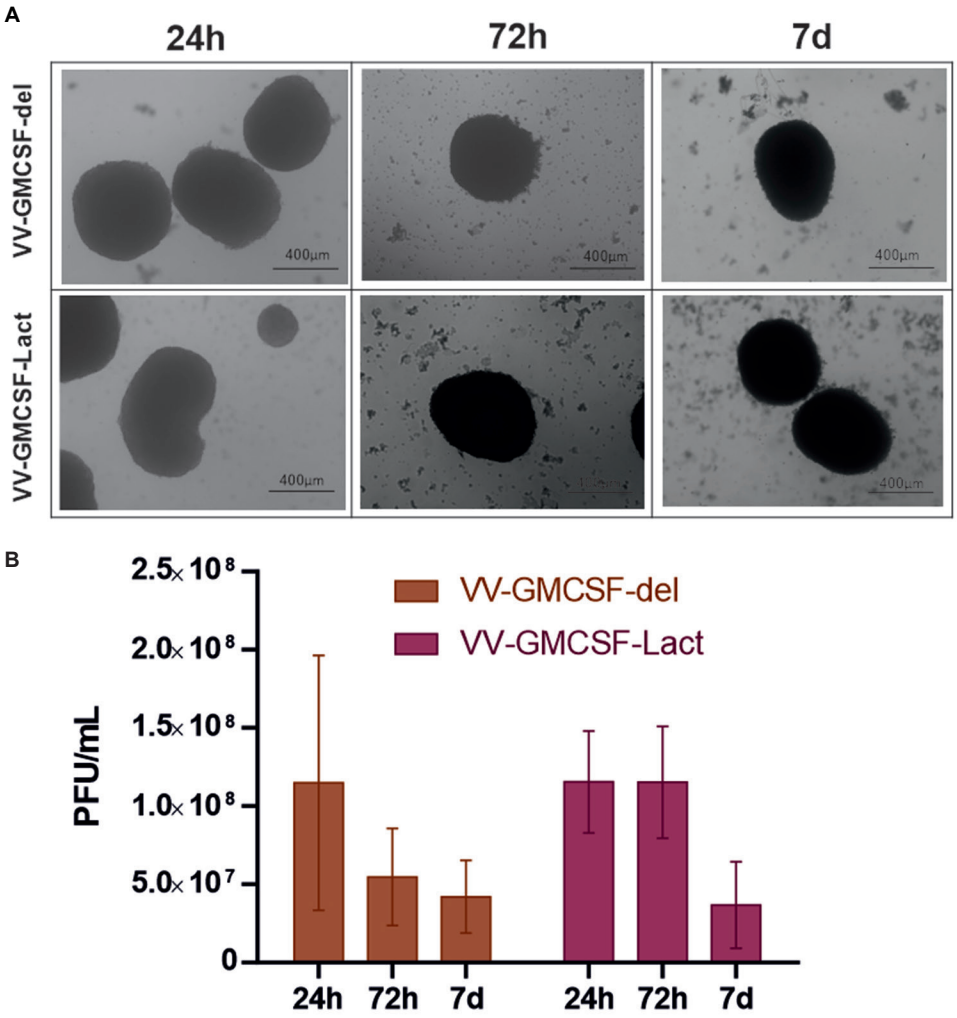

Figure 2. (A) Micrographs of three-dimensional U-87 MG glioblastoma spheroids incubated with VV-GMCSF-Lact and VV-GMCSF-del viruses for 24 h, 72 h, and 7 days (scale bar: 400 µm; magnification: 4×). (B) Viral load in PFU/mL after 24 h, 72 h, and 7 days. Data are presented as mean and standard deviation (n = 18).
Abbreviation: VV-GMCSF: Vaccinia virus-granulocyte–macrophage colony-stimulating factor.

altered in response to infection with an oncolytic virus, both in 3D spheroids and GCOAs (Figure 5A and B).

We observed a significant 2.27-fold decrease in the expression of the *FSCN1* gene, which is associated with tumor cell invasiveness and metastasis,[26] in GCOAs 72 h after infection with VV-GMCSF-Lact. However, no statistically significant changes in gene expression were observed in GCOAs treated with VV-GMCSF-del. In contrast, both recombinant viruses effectively suppressed *FSCN1* expression after 72 h of incubation, with 3- and 1.74-fold decreases in mRNA levels on treatment with VV-GMCSF-del and VV-GMCSF-Lact, respectively. Notably, in 3D spheroids, a significant increase in *FSCN1* gene expression was observed 24 h after viral infection (p<0.01).

The expression profiles of *SCUBE2* differed significantly between 3D spheroids and GCOAs. While *SCUBE2* displayed significant upregulation in 3D spheroids (6.53- and 11-fold) within the first 24 h following VV-GMCSF-del and VV-GMCSF-Lact infection, respectively, we observed a persistent downregulation of the gene in GCOAs throughout the 7-day experiment (1.82-, 2.37-, and 2.64-fold decreases relative to control samples for VV-GMCSF-del at 24 h, 72 h, and 7 days, respectively, and a 2.57-fold decrease at 72 h for VV-GMCSF-Lact.

Remarkably, we observed a persistent decline in expression levels of the *TNFRSF9* gene, a member of the tumor necrosis factor receptor superfamily,[27] in response to viral infection in all analysed 3D spheroids and GCOAs.

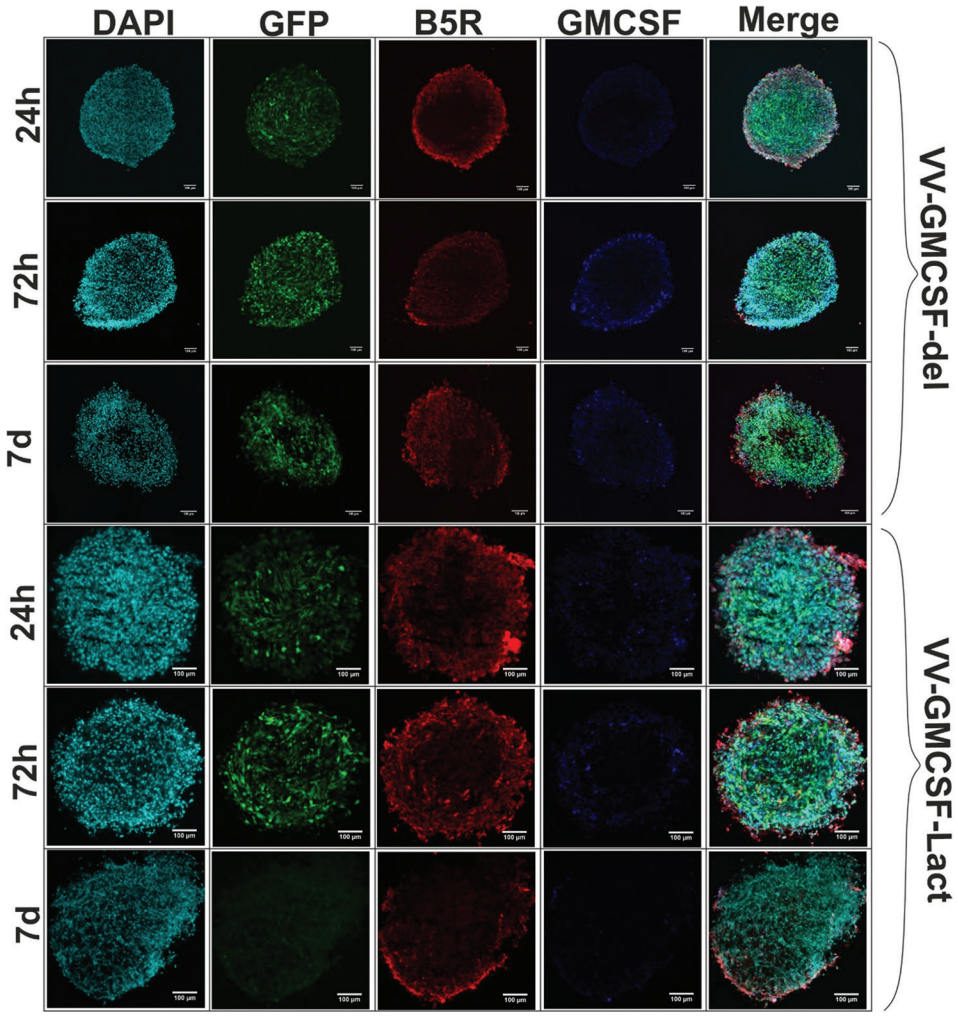

Figure 3. Immunohistochemical analysis of three-dimensional U-87 MG glioblastoma spheroids incubated with VV-GMCSF-del and VV-GMCSF-Lact viruses for 24 h, 72 h, and 7 days using primary antibodies against vaccinia virus B5R and GM-CSF proteins (scale bar: 100 µm; magnification: 20×). Abbreviations: DAPI: 4',6-diamidino-2-phenylindole; GFP: Green fluorescent protein; GMCSF: Granulocyte–macrophage colony-stimulating factor; VV-GMCSF: Vaccinia virus-granulocyte–macrophage colony-stimulating factor.

We also qualitatively assessed the degree of invasion of 3D spheroid U-87 MG glioblastoma and CO using immunohistochemical analysis. On day 10, glioblastoma cells from 3D spheroids began to invade the thickness of the CO (Figure 5C). GCOAs were then infected with both virus strains. Using the B5R envelope protein and *GMCSF* (the transgene inserted into the VV-GMCSF-Lact or VV-GMCSF-del viral genome) (Figure 6), viral markers were visualized in both glioblastoma cells and the crypt regions of the CO, where rapidly dividing cells are located.

4. Discussion

Over the past 50 years, a vast collection of different tumor cell lines has been obtained worldwide.[28] These immortalized cell lines and primary cells are widely used in research because they are easy to culture, can reflect some important features of different cancers, and are also useful for studying the disruption of biochemical pathways in malignant cells. However, instead of adherent tumor cell cultures, more relevant models for studying drugs and mechanisms of carcinogenesis have emerged.[29] For example, several studies have found differences in drug sensitivity between 2D and 3D cultures, both to individual drugs and to combinations of drugs. This may be due to differences in metabolism (the Warburg effect), the presence of concentration gradients of the antitumor drug, oxygen, and nutrients, and the intercellular interactions with the extracellular matrix. These factors make 3D cells more resistant to drug action than adherent cell cultures.[30]

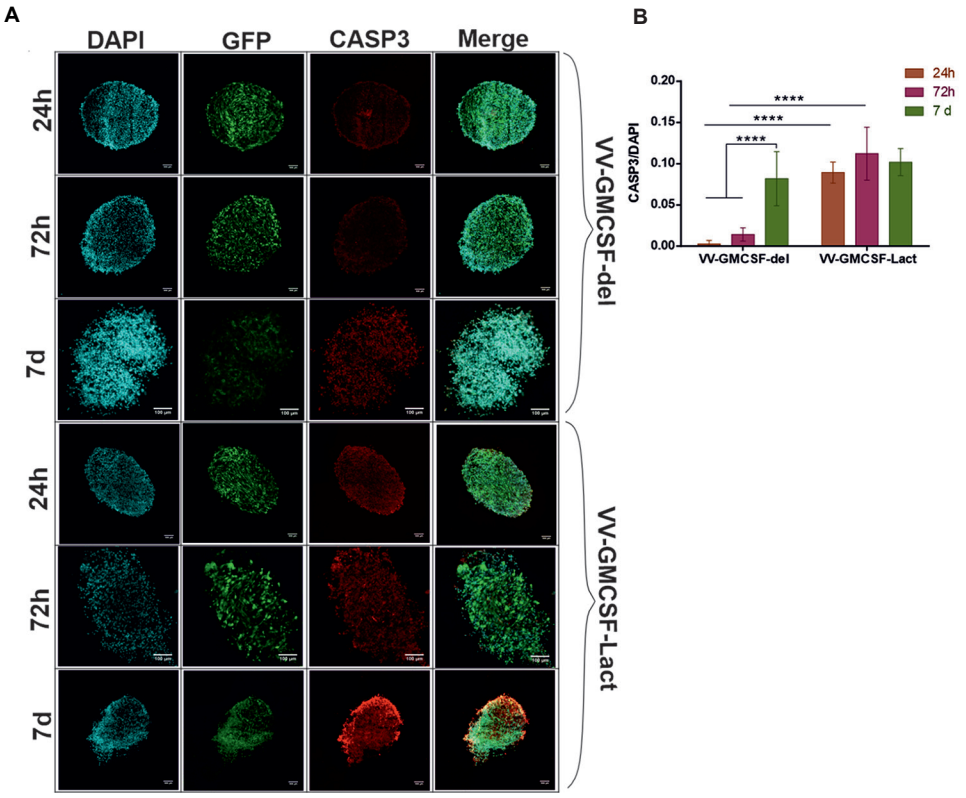

Figure 4. (A) Immunohistochemical analysis of three-dimensional U-87 MG glioblastoma spheroids incubated with VV-GMCSF-del and VV-GMCSF-Lact viruses for 24 h, 72 h, and 7 days (scale bar: 100 µm; magnification: 20×). (B) Percentage of CASP3-positive cells relative to total cells at 24 h, 72 h, and 7 days post-incubation. Data are presented as mean and standard deviation ($n = 9$). ****$p<0.0001$ indicates statistically significant different.
Abbreviations: CASP3: Caspase-3; DAPI: 4',6-diamidino-2-phenylindole; GFP: Green fluorescent protein; VV-GMCSF: Vaccinia virus-granulocyte–macrophage colony-stimulating factor.

Although GCOAs provide a human-specific 3D neuroepithelial architecture that supports physiologically relevant patterns of glioblastoma infiltration, we acknowledge that these models only partially recapitulate the *in vivo* tumor microenvironment. Invasion patterns observed in our GCOAs, including single-cell infiltration and remodeling of adjacent neuroepithelium, are consistent with those described in patient tumors. However, COs lack vasculature, microglia, mature reactive astrocytes, and complete immune signaling, all of which shape glioblastoma progression *in vivo*. We therefore emphasize that GCOAs are well-suited for studying early tumor–brain interactions and evaluating viral cytotoxicity in a human context, but they cannot fully reproduce the complexity of glioblastoma–brain microenvironmental interactions.

Glioblastoma, a highly aggressive Grade IV glioma, has an extremely poor prognosis, with median overall survival ranging from 14 to 20.9 months after initial diagnosis. Genomic, transcriptomic, and epigenomic alterations, the presence of stem cells in the peritumoral zone, and the blood–brain barrier contribute to the resistance of glioblastoma to standard treatments such as radiotherapy and chemotherapy. Consequently, oncolytic virotherapy has emerged as a promising approach, targeting actively dividing cancer cells. Previously, in the Laboratory of Biotechnology at the Institute of Chemical Biology and Fundamental Medicine, Siberian Branch of the Russian Academy of Sciences, in collaboration with the State Research Center of Virology and Biotechnology Vector, a recombinant strain – VV-GMCSF-Lact – was constructed based on the Russian VACV strain L-IVP (GenBank KP233807). The present study aimed to investigate the cytotoxic effects of the oncolytic recombinant VV-GMCSF-Lact compared to VV-GMCSF-del in two 3D glioblastoma models: GCOAs and 3D U-87 MG glioblastoma cell spheroids.

The findings reveal that the cytotoxic efficiency of the VV-GMCSF-Lact strain is higher by almost two orders of magnitude compared with VV-GMCSF-del (Figures 1 and 4). This difference can be explained by the fact that VV-GMCSF-Lact is a double recombinant virus, carrying not only the human *GMCSF* gene but also a gene encoding the oncotoxic protein in lactaptin, which enhances cytotoxicity by inducing apoptosis in tumor cells.

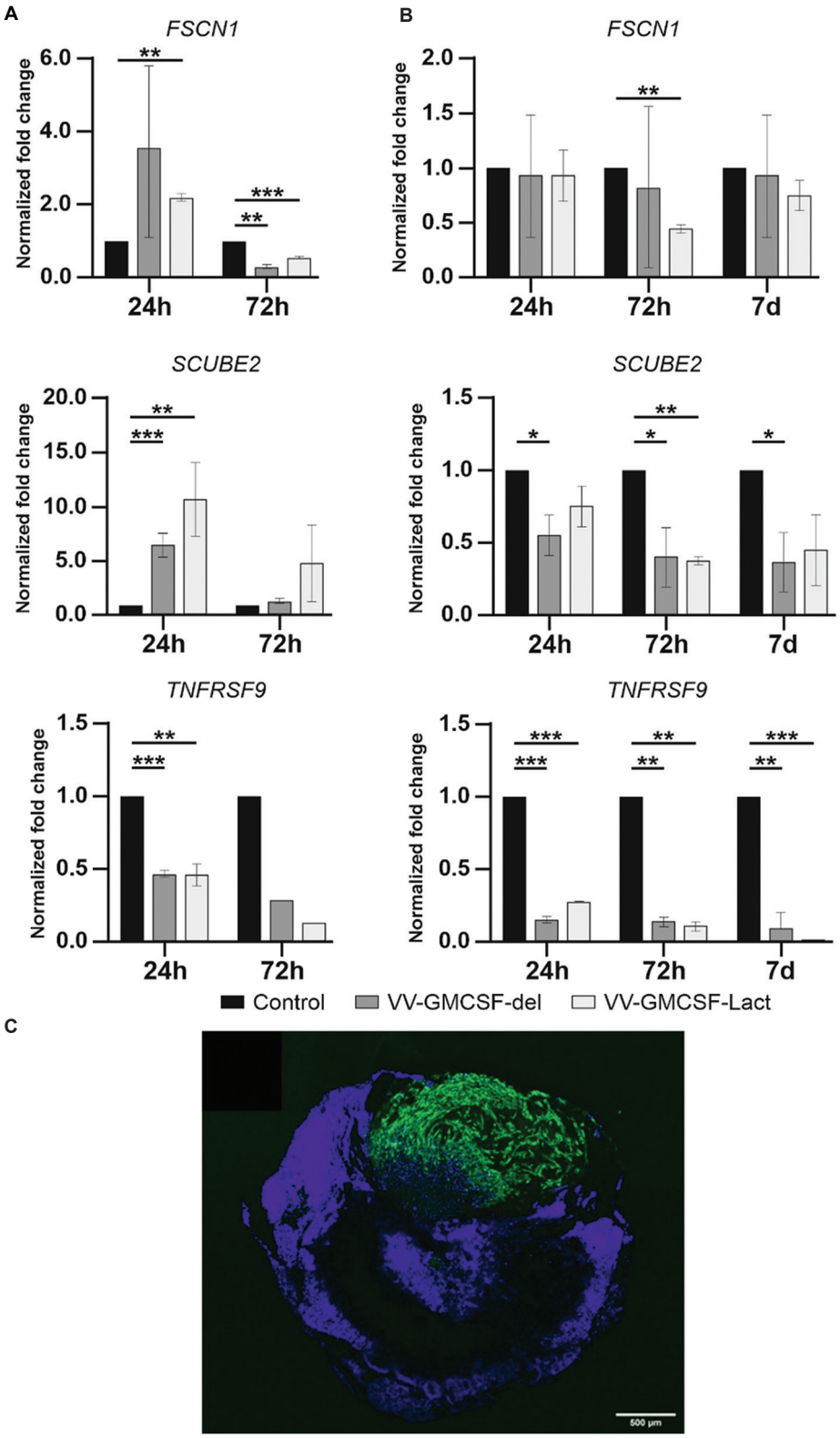

Figure 5. Real-time reverse transcription–polymerase chain reaction results for genes associated with invasion (*FSCN 1, SCUBE 2, TNFRSF9*) in (A) three-dimensional glioblastoma spheroids (A) and (B) glioblastoma–cerebral organoid assembloid (GCOA). Data are presented as mean ± standard deviation ($n = 9$). (C) Immunohistochemical analysis of GCOA on day 10 of co-cultivation (scale bar: 500 µm; magnification: 20×).

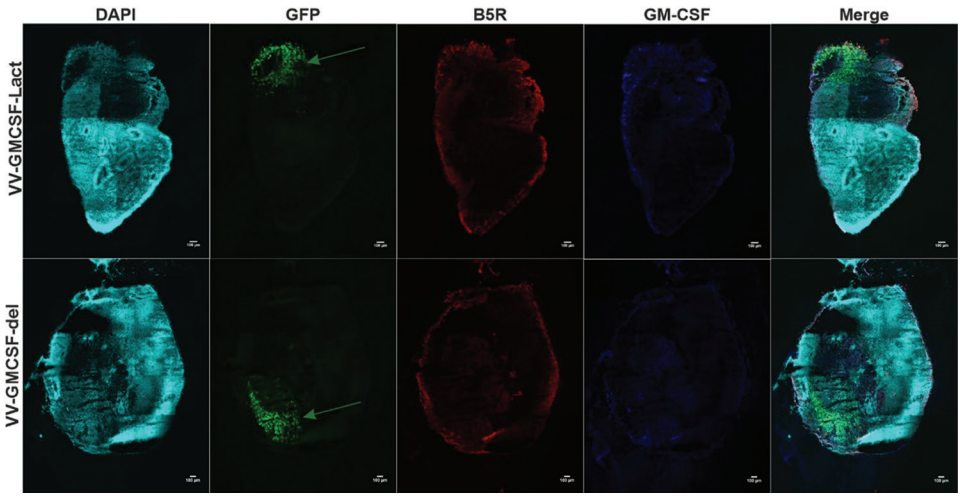

Figure 6. Immunohistochemical analysis of glioblastoma–cerebral organoid assembloid incubated with VV-GMCSF-Lact and VV-GMCSF-del viruses for 72 h, using primary antibodies against vaccinia virus B5R and GM-CSF proteins. Green arrows indicate glioblastoma cell invasion into the thickness of the cerebral organoids (scale bar: 100 μm; magnification: 20×).
Abbreviations: DAPI: 4',6-diamidino-2-phenylindole; GFP: Green fluorescent protein; GM-CSF: Granulocyte–macrophage colony-stimulating factor; VV-GMCSF: Vaccinia virus-granulocyte–macrophage colony-stimulating factor.

Moreover, the viral load in 3D spheroids infected with both strains was similar.

In addition, the findings reveal that the proportion of CASP3-positive cells remained at an approximately constant elevated level at all three time points in the VV-GMCSF-Lact group, whereas in the VV-GMCSF-del group, the proportion of CASP3-positive cells increased only on day 7 post-infection, indicating the greater efficiency of the double recombinant virus. The invasion of glioblastoma cells into the thickness of the CO was observed on day 10. Using immunohistochemical analysis, B5R and GM-CSF viral markers were visualized in both glioblastoma cells and the crypt regions of the CO, where rapidly dividing cells are located. These cells may also have elevated levels of thymidine kinase, which is necessary for viral replication.

Mutations in key genes play a crucial role in gliomagenesis by modulating important signaling pathways, thereby altering critical intracellular processes such as DNA damage and repair, cell proliferation, metabolism, and invasiveness.[31] Oncolytic virotherapy can modulate the post-transcriptional activity of tumor genes, increasing tumor cell sensitivity to viral treatment and reducing cell viability. In our previous studies, we conducted transcriptomic analyses of immortalized and patient-derived glioma adherent cultures treated with VV-GMCSF-Lact, revealing differential expression of genes associated with tumor cell invasion, proliferation, and growth.[32,33] Infection of cancer cells resulted in the suppression of genes involved in cell cycle progression, particularly those regulating spindle organization, sister chromatid segregation, and the G2/M checkpoint.

The findings of the present study demonstrate a decrease in the gene expression of *FSCN1 (*72 h group), *SCUBE2*, and *TNFRSF9* in the GCOA group infected with recombinant viruses compared with control samples. In the 3D spheroid group, a similar trend was observed for *TNSFR9* and *FSCN1* genes (72 h group), with decreased expression relative to the control. In contrast, *SCUBE2* and *FSCN1* exhibited a sharp increase at the 24 h time point.

Fascin proteins are known to assemble F-actin into parallel bundles and are involved in the formation of actin-based cellular protrusions. Consequently, the protein they encode plays a crucial role in cell migration, motility, adhesion, and intercellular interactions.[34] Our previous transcriptome analysis of adherent immortalized and primary glioma cultures incubated with VV-GMCSF-Lact virus showed a decrease in the expression of this gene,[32] which is consistent with the results of the present study for both 3D cultures, but only in the 72 h group ($p<0.01$).

Reduced expression of this gene by the virus supports the antitumor efficacy of virotherapy. *SCUBE2* functions downstream of vascular endothelial growth factor receptor 2 phosphorylation and hypoxia-inducible factor-1α–mediated mitogen-activated protein kinase activation, suggesting a role in angiogenesis.[35,36] In addition, *SCUBE2* has been reported to be involved in inflammatory processes.[37] We previously demonstrated that genes associated with the interferon-γ response, nuclear factor κ-light-chain-enhancer of activated B cells signaling

pathways, and chemokine- and cytokine-mediated inflammation exhibit increased expression on virus exposure.[32] We hypothesize that the increased *SCUBE2* expression in the 3D spheroid group may be related to the presence of a hypoxic core in the neurospheres and its subsequent destruction by the virus. In contrast, in GCOAs, its decreased expression may reflect either the absence of vascular endothelial dysfunction and inflammation or the influence of the virus on hiPSCs, which also contribute to the observed gene expression changes.

Moreover, *TNFRSF9* is considerably upregulated in human gliomas, with predominant expression in perivascular and peritumoral regions, and its decreased expression may promote tumor eradication.[38] In this study, both recombinant viruses reduced *TNFRSF9* expression in 3D spheroids and the GCOAs, consistent with previously obtained transcriptome analysis data from immortalized and primary adherent glioma cell cultures incubated with VV-GMCSF-Lact virus.[32]

Notably, there are several limitations of both the U-87 MG 3D spheroids and GCOA models that should be considered when interpreting our findings. The widely used U-87 MG line is known to exhibit genetic drift and atypical transcriptional patterns compared with primary glioblastoma, which may limit its ability to reproduce tumor heterogeneity and invasion programs fully. Although GCOAs provide a more physiologically relevant human neuroepithelial environment, they also lack essential components of the *in vivo* microenvironment, including vasculature, microglia, reactive astrocytes, and a complete immune signaling network. In addition, the extracellular matrix composition and mechanical properties of COs differ from those of the adult human brain and may influence invasion dynamics and viral susceptibility. Taken together, these factors indicate that each model captures only part of the complexity of glioblastoma biology, and our interpretations reflect the complementary strengths and limitations of both systems.

5. Conclusion

Oncolytic virotherapy has emerged as a promising method for treating tumors. It relies on both the direct lysis of tumor cells by the virus and the induction of a virus-mediated antitumor immune response. The antitumor efficacy of recombinant viruses can be enhanced by integrating genes encoding oncotoxic and immunomodulatory proteins into their genome. This approach is particularly promising for the treatment of glioblastoma, which is characterized by a high degree of invasion and proliferation. 3D glioblastoma spheroids and GCOAs can be employed in the development of antitumor drugs, including recombinant oncolytic viruses. Moreover, both models are well-suited for studying early tumor–brain interactions and evaluating CNS-targeted agents. They possess cytoarchitecture similar to that of actual tumors (especially GCOAs), are relatively easy to handle, and allow for high-throughput screening and scaling. However, they cannot fully recapitulate the complexity of glioblastoma interactions with the brain microenvironment.

Acknowledgments

We would like to thank the Microscopic Center of the Siberian Branch of the Russian Academy of Sciences for granting access to the microscopic equipment.

Funding

This study, including cell viability assays, polymerase chain reaction, immunohistochemistry, and quantitative polymerase chain reaction, was supported by the Russian Science Foundation (Grant No. 22-64-00041; available at https://rscf.ru/project/22-64-00041/, accessed on November 1, 2025). Cell culture maintenance was supported by the Russian state-funded project of the Institute of Chemical Biology and Fundamental Medicine, Siberian Branch of the Russian Academy of Sciences (Grant No.: 125012900932-4).

Conflict of interest

The authors declare they have no competing interests.

Author contributions

Conceptualization: Maya Dymova, Tatiana Shnaider, Vladimir Richter
Formal analysis: Elena Kuligina
Investigation: Maya Dymova, Gleb Petrov, Danil Drokov
Methodology: Maya Dymova, Gleb Petrov, Tatiana Shnaider, Sophia Yakovleva
Writing – original draft: Maya Dymova, Gleb Petrov
Writing – review & editing: Maya Dymova, Gleb Petrov

Ethics approval and consent to participate

Not applicable.

Consent for publication

Not applicable.

Availability of data

Data are available from the corresponding author on reasonable request.

References

1. Bray F, Laversanne M, Sung H, *et al*. Global cancer statistics 2022: GLOBOCAN estimates of incidence and mortality worldwide for 36 cancers in 185 countries. *CA Cancer J Clin*. 2024;74(3):229-263.

   doi: 10.3322/caac.21834

2. Miller KD, Ostrom QT, Kruchko C, *et al*. Brain and other central nervous system tumor statistics, 2021. *CA Cancer J Clin*. 2021;71(5):381-406.

   doi: 10.3322/caac.21693

3. Ma R, Taphoorn MJB, Plaha P. Advances in the management of glioblastoma. *J Neurol Neurosurg Psychiatry*. 2021;92(10):1103-1111.

   doi: 10.1136/jnnp-2020-325334

4. Wu W, Klockow JL, Zhang M, *et al*. Glioblastoma multiforme (GBM): An overview of current therapies and mechanisms of resistance. *Pharmacol Res*. 2021;171:105780.

   doi: 10.1016/j.phrs.2021.105780

5. Gimple RC, Bhargava S, Dixit D, Rich JN. Glioblastoma stem cells: Lessons from the tumor hierarchy in a lethal cancer. *Genes Dev*. 2019;33(11-12):591-609.

   doi: 10.1101/gad.324301.119

6. Vargas López AJ. Glioblastoma in adults: A society for neuro-oncology (SNO) and European society of neuro-oncology (EANO) consensus review on current management and future directions. *Neuro Oncol*. 2021;23(3):502-503.

   doi: 10.1093/neuonc/noaa287

7. Seker-Polat F, Pinarbasi Degirmenci N, Solaroglu I, Bagci-Onder T. Tumor cell infiltration into the brain in glioblastoma: From mechanisms to clinical perspectives. *Cancers (Basel)*. 2022;14(2):443.

   doi: 10.3390/cancers14020443

8. Bose A, Datta S, Mandal R, Ray U, Dhar R. Increased heterogeneity in expression of genes associated with cancer progression and drug resistance. *Transl Oncol*. 2024;41:101879.

   doi: 10.1016/j.tranon.2024.101879

9. Qiu J, Sun M, Wang Y, Chen B. Identification of hub genes and pathways in gastric adenocarcinoma based on bioinformatics analysis. *Med Sci Monit*. 2020;26:e920261.

   doi: 10.12659/msm.920261

10. Kapałczyńska M, Kolenda T, Przybyła W, *et al*. 2D and 3D cell cultures - a comparison of different types of cancer cell cultures. *Arch Med Sci*. 2016;14(4):910-919.

    doi: 10.5114/aoms.2016.63743

11. Paolillo M, Comincini S, Schinelli S. *In vitro* glioblastoma models: A journey into the third dimension. *Cancers (Basel)*. 2021;13(10):2449.

    doi: 10.3390/cancers13102449

12. Heinrich MA, Huynh NT, Heinrich L, Prakash J. Understanding glioblastoma stromal barriers against NK cell attack using tri-culture 3D spheroid model. *Heliyon*. 2024;10(3):e24808.

    doi: 10.1016/j.heliyon.2024.e24808

13. Rybin MJ, Ivan ME, Ayad NG, Zeier Z. Organoid models of glioblastoma and their role in drug discovery. *Front Cell Neurosci*. 2021;15:605255.

    doi: 10.3389/fncel.2021.605255

14. Kelava I, Lancaster MA. Dishing out mini-brains: Current progress and future prospects in brain organoid research. *Dev Biol*. 2016;420(2):199-209.

    doi: 10.1016/j.ydbio.2016.06.037

15. Pine AR, Cirigliano SM, Nicholson JG, *et al*. Tumor microenvironment is critical for the maintenance of cellular states found in primary glioblastomas. *Cancer Discov*. 2020;10(7):964-979.

    doi: 10.1158/2159-8290.cd-20-0057

16. Bian S, Repic M, Guo Z, *et al*. Genetically engineered cerebral organoids model brain tumour formation. *Nat Methods*. 2018;15(8):631-639.

    doi: 10.1038/s41592-018-0070-7

17. Ogawa J, Pao GM, Shokhirev MN, Verma IM. Glioblastoma model using human cerebral organoids. *Cell Rep*. 2018;23(4):1220-1229.

    doi: 10.1016/j.celrep.2018.03.105

18. Weth FR, Peng L, Paterson E, Tan ST, Gray C. Utility of the cerebral organoid glioma 'GLICO' model for screening applications. *Cells*. 2022;12(1):153.

    doi: 10.3390/cells12010153

19. Linkous A, Balamatsias D, Snuderl M, *et al*. Modeling patient-derived glioblastoma with cerebral organoids. *Cell Rep*. 2019;26(12):3203-3211.e5.

    doi: 10.1016/j.celrep.2019.02.063

20. Fedorova V, Pospisilova V, Vanova T, *et al*. Glioblastoma and cerebral organoids: Development and analysis of an *in vitro* model for glioblastoma migration. *Mol Oncol*. 2023;17(4):647-663.

    doi: 10.1002/1878-0261.13389

21. Vasileva N, Ageenko A, Byvakina A, *et al*. The recombinant oncolytic virus VV-GMCSF-lact and chemotherapy drugs against human glioma. *Int J Mol Sci*. 2024;25(8):4244.

    doi: 10.3390/ijms25084244

22. Kochneva G, Sivolobova G, Tkacheva A, *et al*. Engineering of double recombinant vaccinia virus with enhanced

oncolytic potential for solid tumor virotherapy. *Oncotarget*. 2016;7(45):74171-74188.

doi: 10.18632/oncotarget.12367

23. Vasileva N, Ageenko A, Dmitrieva M, *et al*. Double recombinant vaccinia virus: A candidate drug against human glioblastoma. *Life (Basel)*. 2021;11(10):1084.

doi: 10.3390/life11101084

24. Gridina MM, Matveeva NM, Fishman VS, *et al*. Allele-specific biased expression of the *CNTN6* gene in iPS cell-derived neurons from a patient with intellectual disability and 3p26.3 microduplication involving the *CNTN6* gene. *Mol Neurobiol*. 2018;55:6533-6546.

doi: 10.1007/s12035-017-0851-5

25. Yakovleva S, Knyazeva A, Yunusova A, *et al*. Functional divergence of NOTCH1 and NOTCH2 in human cerebral organoids reveals receptor-specific roles in early corticogenesis. *Int J Mol Sci*. 2025;26(15):7309.

doi: 10.3390/ijms26157309

26. Liu H, Zhang Y, Li L, *et al*. Fascin actin-bundling protein 1 in human cancer: Promising biomarker or therapeutic target? *Mol Ther Oncolytics*. 2021;20:240-264.

doi: 10.1016/j.omto.2020.12.014

27. Glorieux C, Huang P. CD137 expression in cancer cells: Regulation and significance. *Cancer Commun (Lond)*. 2019;39(1):70.

doi: 10.1186/s40880-019-0419-z

28. Goodspeed A, Heiser LM, Gray JW, Costello JC. Tumor-derived cell lines as molecular models of cancer pharmacogenomics. *Mol Cancer Res*. 2016;14(1):3-13.

doi: 10.1158/1541-7786.mcr-15-0189

29. Wang X, Sun Y, Zhang DY, Ming GL, Song H. Glioblastoma modeling with 3D organoids: Progress and challenges. *Oxford Open Neurosci*. 2023;6(2):kvad008.

doi: 10.1093/oons/kvad008

30. Keller F, Bruch R, Schneider R, Meier-Hubberten J, Hafner M, Rudolf R. A scaffold-free 3-D Co-culture mimics the major features of the reverse warburg effect *in vitro*. *Cells*. 2020;9(8):1900.

doi: 10.3390/cells9081900

31. Kannan S, Murugan AK, Balasubramanian S, Munirajan AK, Alzahrani AS. Gliomas: Genetic alterations, mechanisms of metastasis, recurrence, drug resistance, and recent trends in molecular therapeutic options. *Biochem Pharmacol*. 2022;201:115090.

doi: 10.1016/j.bcp.2022.115090

32. Semenov DV, Vasileva NS, Dymova MA, *et al*. Transcriptome changes in glioma cells upon infection with the oncolytic virus VV-GMCSF-lact. *Cells*. 2023;12(22):2616.

doi: 10.3390/cells12222616

33. Semenov DV, Vasileva NS, Menyailo ME, *et al*. Single-cell transcriptomic changes in patient-derived glioma and U87 glioblastoma cell cultures infected with the oncolytic virus VV-GMCSF-lact. *Int J Mol Sci*. 2025;26(14):6983.

doi: 10.3390/ijms26146983

34. Lamb MC, Tootle TL. Fascin in cell migration: More than an actin bundling protein. *Biology (Basel)*. 2020;9:403.

doi: 10.3390/biology9110403

35. Guo E, Liu H, Liu X. Overexpression of SCUBE2 inhibits proliferation, migration, and invasion in glioma cells. *Oncol Res*. 2017;25(3):437-444.

doi: 10.3727/096504016x14747335734344

36. Lin YC, Sahoo BK, Gau SS, Yang RB. The biology of SCUBE. *J Biomed Sci*. 2023;30:33.

doi: 10.1186/s12929-023-00925-3

37. Ali H. SCUBE2, vascular endothelium, and vascular complications: A systematic review. *Biomed Pharmacother*. 2020;127:110129.

doi: 10.1016/j.biopha.2020.110129

38. Blank AE, Baumgarten P, Zeiner P, *et al*. Tumour necrosis factor receptor superfamily member 9 (TNFRSF9) is up-regulated in reactive astrocytes in human gliomas. *Neuropathol Appl Neurobiol*. 2014;41(2):e56-e67.

doi: 10.1111/nan.12135